

Collinearity approximations and kinematic shifts in partonic shower algorithms

F. Hautmann^{1,a}, H. Jung²

¹University of Oxford, Physics Department, Oxford OX1 3NP, UK

²Deutsches Elektronen Synchrotron, 22603 Hamburg, Germany

Received: 28 September 2012 / Revised: 5 November 2012 / Published online: 11 December 2012

© The Author(s) 2012. This article is published with open access at Springerlink.com

Abstract We study kinematic effects due to the approximation of on-shell, collinear partons in shower Monte Carlo event generators. We observe that the collinearity approximation, combined with the requirements of energy-momentum conservation, gives rise to a kinematic shift, event by event, in longitudinal momentum distributions. We present numerical results in the case of jet and heavy-flavor production processes measured at the LHC.

1 Introduction

Phenomenological analyses of complex final states produced by hard processes at the Large Hadron Collider (LHC) rely on event simulation by parton shower Monte Carlo generators [1]. These are used both to supplement finite-order perturbative calculations with all-order, leading-logarithmic QCD radiative terms and to incorporate nonperturbative effects from hadronization, multiple parton interactions, underlying events [2–4].

The shower Monte Carlo generators [2–4] treat QCD multi-parton radiation within collinear ordering approximations. These approximations have proved to be very successful for Monte Carlo simulation of final states at LEP and Tevatron. On the other hand at the LHC, unlike previous collider experiments, the phase space opens up for events with multiple hard scales and multiple jets to occur with sizeable rates, while the angular and rapidity coverage of detectors extends over a much wider range. In this case corrections to collinear ordering can significantly affect the structure of multi-jet final states [5–7]. This, for instance, will influence uncertainties [8] of NLO-matched shower calculations [9] for jet observables.

In this letter we investigate effects of kinematic origin arising from collinearity approximations in the parton showering algorithms. While the dynamical corrections studied in [5–7] come from terms beyond NLO in QCD perturbation theory (possibly enhanced in certain regions of phase space), the contributions studied in this paper are not obviously suppressed by powers of the strong coupling. Rather, they correspond to approximations made by showering algorithms in the parton kinematics. They can be discussed already at the level of leading-order and next-to-leading-order [8, 9] shower calculations.

We find that the collinearity approximation, combined with the requirements of energy-momentum conservation, gives rise to a kinematic shift, event by event, in longitudinal momentum distributions. The size of this shift depends on the observable and on the phase space region, but becomes in general non-negligible with increasing rapidities. In Sect. 2 we discuss the physical origin of this effect. In Sect. 3 we present numerical illustrations for jet production and b -flavor production based on NLO event generators. We give concluding remarks in Sect. 4.

2 Longitudinal momentum shifts in parton showers

Consider inclusive jet hadro-production. LHC experiments have measured one-jet cross sections [10–12] over a kinematic range in transverse momentum and rapidity much larger than in any previous collider experiment. Two kinds of comparison of experimental data with standard model theoretical predictions have been carried out. The first is based on NLO calculations [13] supplemented by nonperturbative (NP) corrections estimated from shower Monte Carlo generators [10–12]. This shows that the NLO calculation agrees with data at central rapidities, while increasing deviations are seen with increasing rapidity at large transverse momentum p_T [10].

^ae-mail: hautmann@mail.cern.ch

A second comparison [10] is based on POWHEG calculations [14], in which NLO matrix elements are matched with parton showers [2–4]. This data comparison shows large differences in the high-rapidity region between results obtained by interfacing POWHEG with different shower models [2–4] and different model tunes [15].

The dependence of high-rapidity jet distributions on parton showering effects is discussed in [16–18] based on results [7] from high-energy factorization [19–21]. These results are valid to single-logarithmic accuracy in the jet rapidity and the jet transverse momentum, and resum terms to all orders in the strong coupling α_s . In the approach [7, 16–18] forward jet production is dominated by the scattering of a highly off-shell, low- x parton off a nearly on-shell, high- x parton. As noted in [16–18], this leads to a sizeable fraction of reconstructed jets receiving contribution from final-state partons produced by showering rather than just partons from hard matrix elements.

Let us now consider the NLO-matched shower Monte Carlo calculations in the light of this physical picture. The Monte Carlo first generates hard subprocess events with full four-momentum assignments for the external lines. In particular, the momenta $k_j^{(0)}$ ($j = 1, 2$) of the partons initiating the hard scatter are on shell, and are taken to be fully collinear with the incoming state momenta p_j ,

$$k_j^{(0)} = x_j p_j \quad (j = 1, 2). \tag{1}$$

Next the showering algorithm is applied, and complete final states are generated including additional QCD radiation from the initial-state and final-state parton cascades. As a result of QCD showering, the momenta k_j are no longer exactly collinear,

$$k_j \neq x_j p_j \quad (j = 1, 2). \tag{2}$$

This corresponds to the soft parton being far off shell in the approach [7]. On the other hand, in the NLO shower calculation the transverse momentum carried by partons with k_j is to be compensated by a change in the kinematics of the hard scattering subprocess. By energy-momentum conservation, this implies a reshuffling, event by event, in the longitudinal momentum fractions x_j of the partons scattering off each other in the hard subprocess. The size of the shift in x_j depends on the emitted transverse momenta.

In the next section we illustrate the longitudinal momentum shifts numerically for jet and heavy-flavor production using POWHEG.

3 Numerical results

We consider jet production in the kinematic range [10] and focus on the high-rapidity region. In the top panels of Fig. 1 we plot the distributions in x_j from POWHEG before parton showering and after parton showering for the low- x and

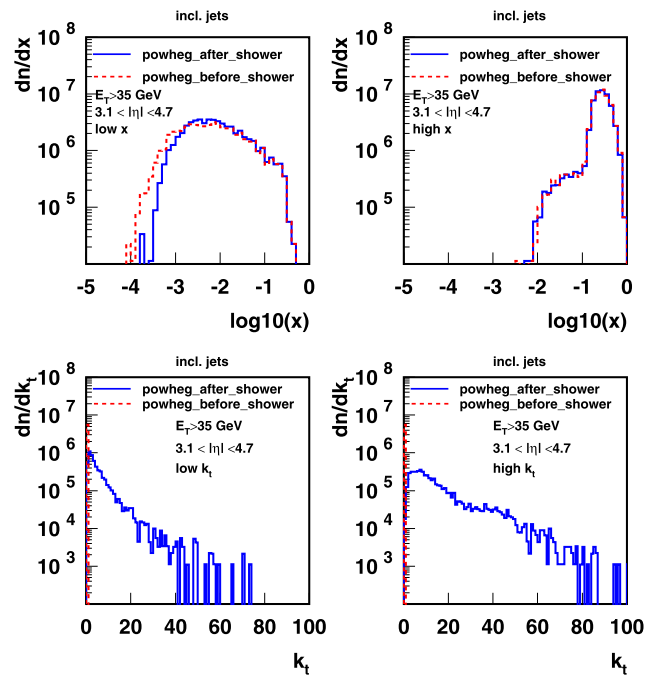


Fig. 1 Distributions in the parton longitudinal momentum fraction x (upper plots) and transverse momentum k_t (lower plots), before and after parton showering, for inclusive jet production at high rapidity

high- x partons. In the bottom panels of Fig. 1 we plot the corresponding distributions in the transverse momentum k_t . The results are obtained using the PYTHIA parton shower tune S0 [15] and CTEQ6M pdfs [22]. They do not include multiple parton interaction and hadronization effects. The kinematic variables in the figure are first calculated for the partons given by POWHEG before shower and then calculated from the PYTHIA event record after shower.

We see from the upper plots in Fig. 1 that the kinematical reshuffling in the longitudinal momentum fraction is negligible for high- x partons but it is significant for low- x partons. This effect characterizes the highly asymmetric parton kinematics [16–18]. We note that in NLO shower calculations, since the perturbative weight for each event is determined by the initial POWHEG simulation, predictions for observables sensitive to this asymmetric region can be affected significantly by the kinematical shift in Fig. 1. Similarly, since the momentum reshuffling is done after evaluation of the parton distribution functions, the kinematical shift can affect predictions also through the pdfs. It will be of interest to examine the impact of this phase space region on total cross sections as well.

The lower plots in Fig. 1 illustrate the distribution of transverse momenta in the initial state as a result of parton showering. We see that this distribution falls off rapidly for the low- k_t initial-state parton, while the distribution for the high- k_t initial-state parton has a significant large- k_t tail. This provides an illustration, at the next-to-leading order, of

the physical picture described in Sect. 2 based on the single-logarithmic, resummed results of [7, 16–18].

Analogous kinematic effects can be examined in the case of bottom-flavor jet production. The LHC measurements of b -jets [23, 24] are reasonably described by NLO-matched shower generators MC@NLO [25] and POWHEG [26] at central rapidities, and they are below these predictions at large rapidity and large p_T . In Fig. 2 we consider b -jets for several different rapidity intervals [23] and plot the gluon x distribution from POWHEG before parton showering and after parton showering. We use the PYTHIA parton shower tune S0 [15], including hadronization. We observe similar shift in longitudinal momentum with increasing rapidity as in the inclusive jet case.

The longitudinal momentum shifts computed in this section may affect parton distribution functions in parton shower calculations. Although we have illustrated the shifts using the event generator POWHEG, the effect is common to other calculation methods using collinear shower algorithms. Further studies of this effect will be reported elsewhere.

4 Conclusions

In this letter we have observed that, in the particular phase space regions for which inclusive jets and b -jets are measured at the LHC, QCD parton showers are sensitive to

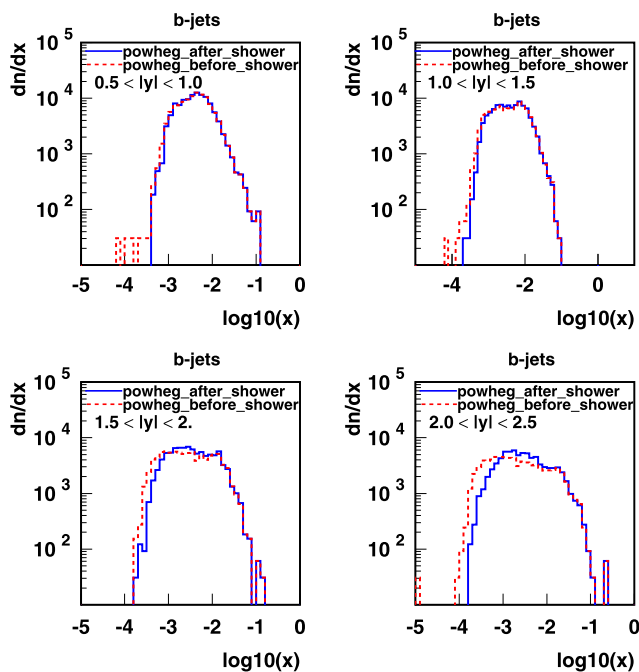


Fig. 2 Production of b -jets: distribution in the parton longitudinal momentum fraction x , before and after parton showering, for different rapidity regions

kinematic corrections associated with approximations of on-shellness and collinearity on the partonic states to which branching algorithms are applied.

Kinematic reshuffling in the longitudinal momentum fractions comes from the implementation of energy-momentum conservation in collinearly ordered showering algorithms. It depends on the emitted transverse momenta, and is present at leading order as well as at next-to-leading order. We have illustrated this effect quantitatively using NLO-matched event generators.

While the effect is generally small for central production if the center-of-mass energy is not too high, we have found that it becomes sizeable in kinematic regions probed by hard production processes at the LHC, for instance jet and heavy-flavor production at high rapidity. These regions have not been accessed experimentally before at previous colliders (e.g., at the Tevatron).

The event-by-event shift in longitudinal momentum distributions affects predictions through both perturbative weights and parton distribution functions. It contributes in particular to the uncertainty on predictions which incorporate results of collinearly ordered showering algorithms.

Formulations that keep track of non-collinear (i.e., transverse and/or anti-collinear) momentum components using unintegrated parton distributions [27–33] will be helpful to take account of the kinematic effect of longitudinal momentum shifts. It will also be of interest to investigate the relative size of the kinematic contribution studied in this article with respect to high-energy dynamical [5–7] effects on jet final states which can be included by unintegrated formalisms.

Open Access This article is distributed under the terms of the Creative Commons Attribution License which permits any use, distribution, and reproduction in any medium, provided the original author(s) and the source are credited.

References

1. See S. Höche, SLAC preprint SLAC-PUB-14498 (2011), for a recent review
2. T. Sjöstrand, S. Mrenna, P. Skands, J. High Energy Phys. **0605**, 026 (2006)
3. G. Corcella et al., J. High Energy Phys. **0101**, 010 (2001). [arXiv:hep-ph/0011363](https://arxiv.org/abs/hep-ph/0011363)
4. G. Corcella et al., [arXiv:hep-ph/0210213](https://arxiv.org/abs/hep-ph/0210213)
5. G. Marchesini, B.R. Webber, Nucl. Phys. B **386**, 215 (1992)
6. F. Hautmann, H. Jung, J. High Energy Phys. **0810**, 113 (2008)
7. M. Deak et al., J. High Energy Phys. **0909**, 121 (2009). [arXiv:0908.1870](https://arxiv.org/abs/0908.1870)
8. S. Höche, M. Schönherr, [arXiv:1208.2815](https://arxiv.org/abs/1208.2815) [hep-ph]
9. P. Nason, B.R. Webber, [arXiv:1202.1251](https://arxiv.org/abs/1202.1251) [hep-ph]
10. G. Aad et al. (ATLAS Coll.), Phys. Rev. D **86**, 014022 (2012)
11. S. Chatrchyan et al. (CMS Coll.), Phys. Rev. Lett. **107**, 132001 (2011)
12. S. Chatrchyan et al. (CMS Coll.), Preprint CMS PAS QCD-11-004
13. Z. Nagy, Phys. Rev. D **68**, 094002 (2003)

14. S. Alioli et al., *J. High Energy Phys.* **1104**, 081 (2011)
15. P.Z. Skands, *Phys. Rev. D* **82**, 074018 (2010)
16. M. Deak et al., *Eur. Phys. J. C* **72**, 1982 (2012)
17. M. Deak et al., [arXiv:1012.6037](https://arxiv.org/abs/1012.6037) [hep-ph]
18. M. Deak et al., [arXiv:1206.7090](https://arxiv.org/abs/1206.7090) [hep-ph]
19. S. Catani et al., *Phys. Lett. B* **242**, 97 (1990)
20. S. Catani et al., *Nucl. Phys. B* **366**, 135 (1991)
21. S. Catani et al., *Phys. Lett. B* **307**, 147 (1993)
22. J. Pumplin et al., *J. High Energy Phys.* **0207**, 012 (2002)
23. S. Chatrchyan et al. (CMS Coll.), *J. High Energy Phys.* **1204**, 084 (2012)
24. G. Aad et al. (ATLAS Coll.), *Eur. Phys. J. C* **71**, 1846 (2011)
25. S. Frixione, P. Nason, B.R. Webber, *J. High Energy Phys.* **0308**, 007 (2003)
26. S. Frixione, P. Nason, G. Ridolfi, *J. High Energy Phys.* **0709**, 126 (2007)
27. P.J. Mulders, *Pramana* **72**, 83 (2009)
28. P.J. Mulders, T.C. Rogers, [arXiv:1102.4569](https://arxiv.org/abs/1102.4569) [hep-ph]
29. F. Hautmann, *Acta Phys. Pol. B* **40**, 2139 (2009)
30. F. Hautmann, *Phys. Lett. B* **655**, 26 (2007)
31. F. Hautmann, H. Jung, [arXiv:0712.0568](https://arxiv.org/abs/0712.0568)
32. E. Avsar, [arXiv:1203.1916](https://arxiv.org/abs/1203.1916) [hep-ph]
33. E. Avsar, [arXiv:1108.1181](https://arxiv.org/abs/1108.1181) [hep-ph]